Viscous Effects in the Elastodynamics of Thick Beams

A. R. Johnson[1] and A. Tessler
Computational Structures Branch
NASA Langley Research Center, MS240
Hampton, VA 23681-0001

Summary

A viscoelastic higher-order thick beam finite element formulation is extended to include elastodynamic deformations. The material constitutive law is a special differential form of the Maxwell solid. In the constitutive model, the elastic strains and the conjugate viscous strains are coupled through a system of first-order ordinary differential equations. The total time-dependent stress is the superposition of its elastic and viscous components. The elastodynamic equations of motion are derived from the virtual work principle. Computational examples are carried out for a thick orthotropic cantilevered beam. A quasi-static relaxation problem is employed as a validation test for the elastodynamic algorithm. The elastodynamic code is demonstrated by analyzing the damped vibrations of the beam which is deformed and then released to freely vibrate.

Introduction

The combination of highly viscous low-modulus materials with the traditional high-modulus materials produces stiff, highly damped load carrying structures. The quasi-static and dynamic analyses of such structures require improvements in the material damping representation over the velocity proportional damping schemes. Halpin and Pagano[1] demonstrated that the relaxation moduli for anisotropic solids produce symmetric matrices that can be expanded in a Prony series form (i.e., a series of exponentially decaying terms). Early viscoelastic models for small deformations of composites focused on computing the complex moduli for anisotropic solids from the elastic properties of the fibers and the complex modulus properties of the matrix.[2,3] Recently, various classical constitutive models have been used including generalized Maxwell and Kelvin-Voigt solids.[4,5] These constitutive models have practical value since they provide adequate approximations for the dynamic softening and hysteresis effects – the phenomena that are not directly proportional to strain rates.

Coleman and Noll[6] and Schapery[7] presented comprehensive discussions on the history integral form of the Maxwell solid. Johnson and Stacer[8] developed a

[1] Vehicle Technology Center, Army Research Laboratory.

differential form of the Maxwell solid constitutive law for large strain viscoelastic deformations of rubber. The formulation required additional viscous strain variables that are conjugate to the elastic strains. The same constitutive law was used by Johnson et al.[9,10] to formulate a viscoelastic, large-displacement shell finite element. In the work of Johnson and Tessler,[11] the differential constitutive law was implemented within Tessler's[12] higher-order beam theory, giving rise to a quasi-static viscoelastic thick beam finite element formulation. They presented several quasi-static numerical solutions demonstrating the relaxation, creep, and cyclic creep response of thick beams. They demonstrated that only minor modifications to an elastic finite element code are needed to produce a computationally efficient viscoelastic code.

In this paper, the quasi-static viscoelastic formulation of Johnson and Tessler[11] is extended to elastodynamics. The mass matrix for the higher-order beam is derived and a modified Newmark algorithm is employed to integrate the equations of motion. The modified Newmark algorithm contains an implicit trapezoidal integration scheme which enables accurate integration of the first-order differential equations for the viscous strains.

Viscoelastic Higher-Order Beam

In this section, an internal variable formulation for a Maxwell solid higher-order beam theory[11] is outlined. The beam dimensions and sign convention are shown in Figure 1. The differential form of the viscoelastic constitutive model for the beam is written in matrix form as

$$\mathbf{s}(t) = \mathbf{C}\mathbf{e} + {}^{*}\mathbf{C}\sum_{n=1}^{N} {}^{*}_{n}\mathbf{e}(t) \tag{1}$$

$${}^{*}_{n}\dot{\mathbf{e}} + {}^{*}_{n}\mathbf{e}/\tau_n = \dot{\mathbf{e}} \qquad \text{for each } n \tag{2}$$

where $\mathbf{s}^T = (\sigma_{xx},\ \sigma_{zz},\ \tau_{xz})$, $\mathbf{e}^T = (\varepsilon_{xx},\ \varepsilon_{zz},\ \gamma_{xz})$, ${}^{*}_{n}\mathbf{e}^T = ({}^{*}_{n}\varepsilon_{xx},\ {}^{*}_{n}\varepsilon_{zz},\ {}^{*}_{n}\gamma_{xz})$

$$\mathbf{C} = \begin{bmatrix} C_{11} & C_{13} & 0 \\ C_{13} & C_{33} & 0 \\ 0 & 0 & C_{55} \end{bmatrix} \quad \text{and} \quad {}^{*}\mathbf{C} = \begin{bmatrix} {}^{*}C_{11} & {}^{*}C_{13} & 0 \\ {}^{*}C_{13} & {}^{*}C_{33} & 0 \\ 0 & 0 & {}^{*}C_{55} \end{bmatrix}$$

The vectors $\mathbf{s}$ and $\mathbf{e}$ are the engineering stresses and strains. The vectors ${}^{*}_{n}\mathbf{e}$ ($n = 1,2,...,N$) are the internal variables, i.e., conjugate viscous strains, where N is the number of terms in a Prony series representation of the material's stress

relaxation response. The matrices $\mathbf{C}$ and ${}^{*}\mathbf{C}$ contain the elastic and viscous stiffness coefficients. In the higher-order beam theory,[12] the components of the displacement vector are approximated through the beam thickness by way of five kinematic variables, i.e.,

$$u_x(x,z,t) = u(x,t) + h\zeta\theta(x,t) \tag{3}$$

$$u_z(x,z,t) = w(x,t) + \zeta w_1(x,t) + \left(\zeta^2 - \frac{1}{5}\right) w_2(x,t) \tag{4}$$

where $\zeta = z/h$ denotes a nondimensional thickness coordinate and $2h$ is the total thickness. The function $u(x,t)$ represents the midplane (i.e. reference plane) axial displacement, $\theta(x,t)$ is the bending rotation of the cross-section of the beam, $w(x,t)$ is the weighted-average deflection, and $w_1(x,t)$ and $w_2(x,t)$ are the higher-order transverse displacement variables enabling a parabolic distribution of $u_z(x,z,t)$ through the thickness.

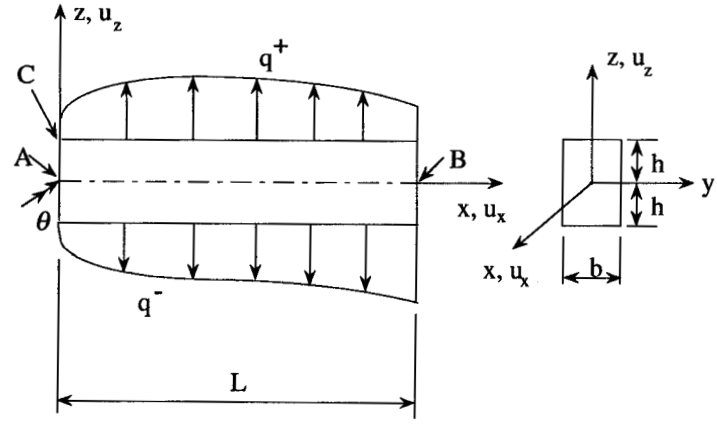

Figure 1. Thick-beam geometry, kinematics, and loading.

The above displacement assumptions give rise to the following thickness distributions for the strains: a linear axial strain, a cubic transverse normal strain, and a quadratic transverse shear strain. These strain components have the following form

$$\varepsilon_{xx} = u(x,t)_{,x} + h\zeta\theta(x,t)_{,x} \tag{5}$$

$$\varepsilon_{zz} = \frac{w_1(x,t)}{h} + \phi_z(\zeta)\,\frac{w_2(x,t)}{h^2} + \phi_x(\zeta)\,\theta(x,t)_{,x} \tag{6}$$

$$\gamma_{xz} = \phi_{xz}(\zeta)\left(w(x,t)_{,x} + \theta(x,t)\right) \tag{7}$$

where $\phi_x(\zeta) = hv_{13}\zeta\left(4-7\zeta^2\right)/17$, $\phi_z(\zeta) = 14\zeta h\left(3-\zeta^2\right)/17$, $\phi_{xz}(\zeta) = 5\left(1-\zeta^2\right)/4$,

and v_{13} is Poisson's ratio. The simplest finite element approximation of this beam theory involves a three-node configuration (see Figure 2) which is achieved by the following interpolations

$$\begin{aligned} &u(\eta,t) = (1-\eta)u_0^\ell(t) + \eta u_1^\ell(t), \quad \theta(\eta,t) = (1-\eta)\theta_0^\ell(t) + \eta\theta_1^\ell(t), \\ &w(\eta,t) = (1-\eta)w_0^\ell(t) + \eta w_1^\ell(t) - \frac{\ell}{2}\eta(1-\eta)\left(\theta_0^\ell(t) - \theta_1^\ell(t)\right), \\ &w_1(\eta,t) = W_1^\ell(t), \quad w_2(\eta,t) = W_2^\ell(t) \end{aligned} \tag{8}$$

where $\eta = x/\ell$ is the nondimensional axial coordinate. The nodal degrees-of-freedom at the two ends of the element are subscripted with indices 0 and 1. Since the strains do not possess derivatives of the $w_1(\eta,t)$ and $w_2(\eta,t)$ variables, these variables need not be continuous at the element nodes and, hence, their simplest approximation is constant for each element. Their corresponding degrees-of-freedom are attributed to a node at the element midspan.

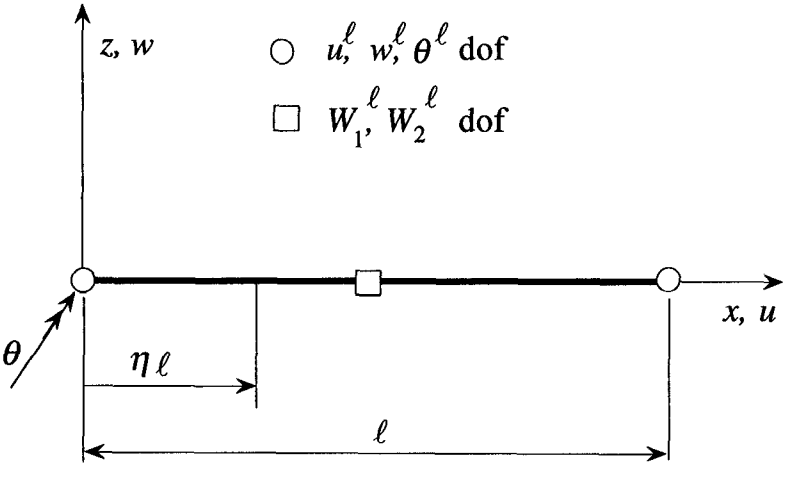

Figure 2. A three-node, higher-order theory thick-beam element.

For dynamic loading, the virtual work statement for an element of volume V with the differential Maxwell constitutive law can be written as

$$\int \rho(\ddot{u}_x\delta u_x + \ddot{u}_z\delta u_z)\,dV + \int \mathbf{e}^T\mathbf{C}\delta\mathbf{e}\,dV + \sum_{n=1}^{N}\int {}^*_n\mathbf{e}^T\,{}^*\mathbf{C}\,\delta\,{}^*_n\mathbf{e}\,dV - \delta W = 0 \tag{9}$$

where the first integral represents the virtual work done by inertial forces, the second is the internal virtual work done by the elastic stresses, the third is the internal virtual work done by the viscous stresses, and δW is the virtual work done by the external forces. Introducing (8) into (3)-(4) and substituting the results into (5)-(7) yields finite element approximations of the strains in terms of the nodal variables, i.e.,

$$\mathbf{e} = \mathbf{B}\mathbf{u}\,, \tag{10}$$

$$\mathbf{B} = \begin{bmatrix} -\frac{1}{\ell} & 0 & -\frac{z}{\ell} & 0 & 0 & \frac{1}{\ell} & 0 & \frac{z}{\ell} \\ 0 & 0 & -\frac{\phi_x}{\ell} & \frac{1}{h} & \frac{\phi_z}{h^2} & 0 & 0 & \frac{\phi_x}{\ell} \\ 0 & -\frac{\phi_{xz}}{\ell} & \frac{\phi_{xz}}{2} & 0 & 0 & 0 & \frac{\phi_{xz}}{\ell} & \frac{\phi_{xz}}{2} \end{bmatrix} \tag{11}$$

and $\mathbf{u}^T = (u_0, w_0, \theta_0, W_1, W_2, u_1, w_1, \theta_1)^\ell$ denotes the element nodal displacement vector. Next, a set of analogous nodal variables, ${}^*_n\mathbf{u}$, and corresponding viscous strains, ${}^*_n\mathbf{e}$, are introduced. These are related by

$${}^*_n\mathbf{e} = \mathbf{B}\,{}^*_n\mathbf{u} \tag{12}$$

The ${}^*_n\mathbf{u}$ variables, which carry the time dependent information for the material within the element, are independent from element to element. The displacements u_x and u_z are then expressed in terms of the element nodal degrees-of-freedom using (3), (4) and (8), giving rise to $u_x = \Phi_x^{\mathrm{T}}\mathbf{u}$ and $u_z = \Phi_z^{\mathrm{T}}\mathbf{u}$, where $\Phi_x(\zeta,\eta)$ and $\Phi_z(\zeta,\eta)$ are vectors of the interpolation functions. The virtual work statement for an element then becomes

$$\begin{aligned} &\ddot{\mathbf{u}}^T \int \rho\left(\Phi_x\Phi_x^T + \Phi_z\Phi_z^T\right) dV\, \delta\mathbf{u} + \mathbf{u}^T \int \mathbf{B}^T\mathbf{C}\,\mathbf{B}\, dV\, \delta\mathbf{u} \\ &\quad + \sum_{n=1}^{N} {}^*_n\mathbf{u}^T \int \mathbf{B}^{T\,*}\mathbf{C}\,\mathbf{B}\, dV\, \delta\,{}^*_n\mathbf{u} - \delta W = 0 \end{aligned} \tag{13}$$

By defining the integrals in (13) as the mass, $\mathbf{m}$, elastic stiffness, $\mathbf{k}$, and viscous stiffness, ${}^*\mathbf{k}$, matrices, there results

$$\left[\ddot{\mathbf{u}}^T\mathbf{m}+\mathbf{u}^T\mathbf{k}\right]\delta\mathbf{u}+\left[\sum_{n=1}^{N}{}^*_n\mathbf{u}^T\,{}^*\mathbf{k}\right]\delta\,{}^*_n\mathbf{u}-\delta W=0 \tag{14}$$

Since $\delta\mathbf{u}=\delta^*_n\mathbf{u}$ when t is constant, the virtual work takes on a simpler form

$$\left[\ddot{\mathbf{u}}^T\mathbf{m}+\mathbf{u}^T\mathbf{k}+\sum_{n=1}^{N}{}^*_n\mathbf{u}^T\,{}^*\mathbf{k}\right]\delta\mathbf{u}-\delta W=0 \tag{15}$$

This implies that at any time t the element equilibrium equations are

$$\mathbf{m}\ddot{\mathbf{u}}+\mathbf{k}\,\mathbf{u}=\mathbf{f}-\sum_{n=1}^{N}{}^*\mathbf{k}\,{}^*_n\mathbf{u} \qquad \text{for each element} \tag{16}$$

where $\mathbf{f}$ denotes the element consistent load vector due to the external loading. Introducing (10) and (12) into the differential equations for the strain variables in (2) yields

$${}^*_n\dot{\mathbf{u}}+{}^*_n\mathbf{u}/\tau_n=\dot{\mathbf{u}} \qquad \text{for each } n \tag{17}$$

The global equilibrium equations are determined by the standard assembly of the element equations, (16). Note, there is no assembly for (17). The global equations of motion are

$$\mathbf{M}\ddot{\mathbf{u}}_g+\mathbf{K}\mathbf{u}_g=\mathbf{F}_{mech}-\mathbf{F}_{visc} \tag{18}$$

where $\mathbf{u}_g$ denotes the global nodal variable vector, $\mathbf{M}$ is the mass matrix, $\mathbf{K}$ is the elastic stiffness matrix, $\mathbf{F}_{mech}$ is the global force vector due to mechanical loads, and $\mathbf{F}_{visc}$ is the assembled vector for $\sum_{n=1}^{N}{}^*\mathbf{k}\,{}^*_n\mathbf{u}$. The viscoelastic problem is solved by simultaneously integrating the first order differential equations, (17), and the second order equations, (18), where the latter is subject to the appropriate boundary restraints.

As far as the finite element implementation is concerned, a conventional linear elastic code can be readily adapted to perform a dynamic analysis for a structure made from a Maxwell material, i.e., a material whose relaxation stiffness coefficients can be modeled with a Prony series. First, the viscous stiffness

coefficients, ${}^{*}C_{ij}$, are used in place of the elastic values to compute the element viscous stiffness matrices, ${}^{*}\mathbf{k}$, which are stored for repeated use. The internal nodal variables for each element, ${}^{*}_{n}\mathbf{u}$, are set equal to their initial values. A modified Newmark algorithm is then used to integrate (18). The modification is required so that (17), stiff relaxation equations, are implicitly integrated.

Applications

Two numerical solutions representative of quasi-static and free vibration deformations of a cantilevered thick orthotropic beam are presented. The beam dimensions are as follows: $L = 0.1\text{m}$, $2h = 0.02\text{m}$, and $b = 1.0\text{m}$ (refer to Figure 1). The beam elastic stiffness coefficients for the state of plane stress can be written in terms of engineering material constants as

$$C_{11} = E_x/(1-\nu_{xz}\nu_{zx}),\ C_{33} = E_z/(1-\nu_{xz}\nu_{zx}),\ C_{13} = \nu_{xz}C_{33},\quad C_{55} = G_{xz}$$

A unidirectional E-glass/epoxy laminate is considered for which the material constants are: $E_x = 38.6$ GPa, $E_z = 8.27$ GPa, $G_{xz} = 4.14$ GPa, $\nu_{xz} = 0.26$, and $\rho = 1.8$ g/cm^3. The viscous relaxation properties are computed from complex modulus versus frequency data for the E-glass/epoxy.[13] The equations for the real and imaginary parts of the effective modulus for a ten term Maxwell solid[14] are least-squares fit to the measured data in a frequency range of 45 Hz – 145 Hz. The least squares minimization was performed using a quadratic programming method that enforced the constraint that each of the moduli in the Maxwell solid must be positive. The time constants for the ten terms are; $\tau_n = 10^{-4}$, $10^{-3.5}$, 10^{-3}, $10^{-2.5}$, 10^{-2}, ... , 10^{1}, and infinity. The resulting Maxwell solid had its moduli scaled so that its equivalent nondimensional Prony series has the form

$$P(t) = 1.0 + 0.01755\, e^{-0.0001t} + 0.000257\, e^{-0.01t} + 0.072014\, e^{-0.3162t}$$

The time dependent stiffness values for the E-glass/epoxy are then given by ${}^{*}\mathbf{C} = P(t)\,\mathbf{C}$.

Example 1. A cantilever beam (reference Figure 1) with w, u, θ fixed at point A has a prescribed deflection w at point B that is ramped from 0 to -1 cm in 0.05 sec and then held constant at -1 cm. Figure 3 depicts the maximum axial stress at point C as a function of time. Also shown are the elastic and viscous stress components comprising the total stress. The decay of the total viscoelastic stress

to its elastic value as time is increased demonstrates the expected step-strain relaxation behavior. Note, when this problem is solved with a velocity proportional viscous damping model the viscous stress for time greater than 0.05 sec is zero.

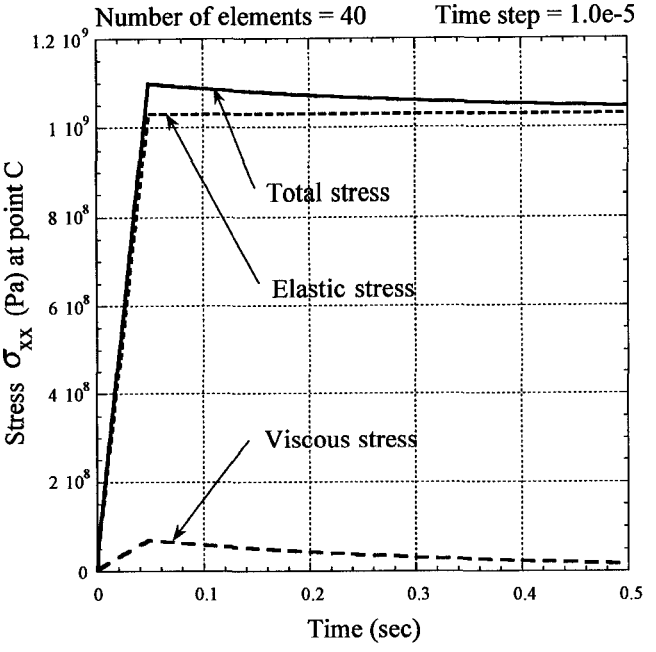

Figure 3. Cantilevered beam under prescribed tip deflection. Stress in top surface at support (point C).

Example 2. The cantilevered beam of Example 1 has its tip (point B) released at t = 0.1 sec and is allowed to vibrate freely thereafter. The resulting tip deflection as a function of time is shown in Figure 4. Figure 5 depicts the value of the dynamic axial stress at point C as a function of time. Note that both relaxation and damped vibration response are obtained within the same finite element solution.

Conclusions

An elastodynamic formulation, which includes a differential form of the Maxwell viscous solid constitutive theory, has been implemented in a higher-order-theory beam finite element. The attractive features of the formulation include: (1) The constitutive constants are the same as those needed in the classical history-integral model, and they are also readily available from step-strain relaxation tests, (2) The internal variables are conjugate to the elastic strain

measures; hence, they are consistent with the kinematic assumptions of the elastic formulation, (3) The update of the state variables can be performed in a parallel computing environment, allowing the viscous force vector in the equations of motion to be determined efficiently within the modified Newmark algorithm,

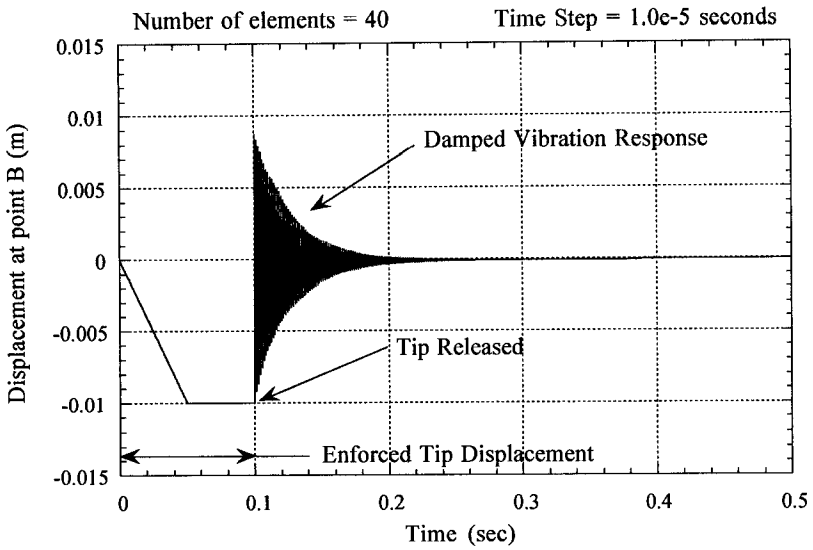

Figure 4. Cantilevered beam under prescribed tip deflection.
Tip released - vibration of tip (Point B).

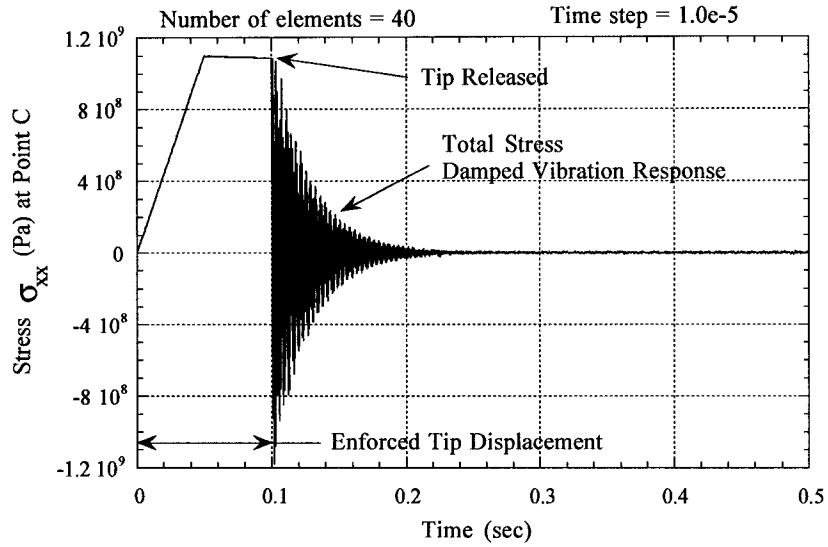

Figure 5. Cantilevered beam under prescribed tip deflection.
Tip released - Stress on top surface at support. (Point C).

(4) Applications of time-dependent displacements and loads are performed within the same finite element algorithm, and (5) The higher-order beam theory accounts for both transverse shear and transverse normal deformations — the effects that need to be accounted for in thick and highly orthotropic beams, and in high-frequency dynamics.

Example 2, in which a quasi-static enforced deformation is followed by a high frequency free vibration, demonstrates the capability of this finite element formulation to simulate physically important phenomena that is computationally difficult to obtain.

Acknowledgment: The authors would like to thank Mr. Michael Dambach, of The George Washington University at the NASA Langley Research Center, for his help in the computational effort.

References

1. Halpin, J. C., and Pagano, N. J., Observations on linear anisotropic viscoelasticity, J. Composite Materials, **2**, No. 1, 68-80 (1968).
2. Hashin, Z., Complex moduli of viscoelastic composites - I. General theory and applications to particulate composites, Int. J. Solids Structures, **6**, 539-552 (1970).
3. Hashin, Z., Complex moduli of viscoelastic composites - II. Fiber reinforced materials, Int. J. Solids and Structures, **6**, 797-807 (1970).
4. Argyris, J., St. Doltsinis, I., and da Silva, V. D., Constitutive modeling and computation of non-linear viscoelastic solids, Part I. Rheological models and numerical integration techniques, Comput. Methods Appl. Mech. Engrg., **88**, 135-163 (1991).
5. Shaw, S., Warby, M. K., and Whiteman, J. R., Numerical techniques for problems of quasistatic and dynamic viscoelasticity, in "The Mathematics of Finite Elements and Applications," edited by J. R. Whiteman, John Wiley & Sons (1994).
6. Coleman, B. D., and Noll, W., Foundations of linear viscoelasticity, Reviews of Modern Physics, **33**, No.2, 239-249 (1961).
7. Schapery, R. A., Viscoelastic behavior and analysis of composite materials, in "Composite Materials", **2**, edited by G. P. Sendeckyj, Academic Press (1974).
8. Johnson, A. R., and Stacer, R. G., Rubber viscoelasticity using the physically constrained system's stretches as internal variables, Rubber Chemistry and Technology, **66**, No.4, 567-577 (1993).

9. Johnson, A. R., Tanner, J. A., and Mason, A. J., A kinematically driven anisotropic viscoelastic constitutive model applied to tires, in "Computational Modeling of Tires," compiled by A. K. Noor and J. A. Tanner, NASA Conference Publication 3306, August 1995.
10. Johnson, A. R., Tanner, J. A., and Mason, J. A., A viscoelastic model for tires analyzed with nonlinear shell elements, presented at the Fourteenth Annual Meeting and Conference on Tire Science and Technology, University of Akron, March 1995.
11. Johnson, A. R., and Tessler, A., A viscoelastic higher-order beam finite element, NASA TM 110260, June 1996.
12. Tessler, A., A two-node beam element including transverse shear and transverse normal deformations, Int. J. for Numer. Methods Eng., **32**, 1027-1039 (1991).
13. Gibson, R. F., and Plunkett, R., Dynamic mechanical behavior of fiber-reinforced composites: Measurement and analysis, J. Composite Materials, **10**, 325-341 (1976).
14. Aklonis, J. J., MacKnight, W. J., and Shen, M., *Introduction to Polymer Viscoelasticity*, John Wiley & Sons, 1972.